

Supporting Information

The Molecular Basis for Dual Fatty Acid Amide Hydrolase (FAAH)/Cyclooxygenase (COX) Inhibition

Giulia Palermo,^[a] Angelo D. Favia,^[a] Marino Convertino,^[a] and Marco De Vivo*^[a, b]

cmdc_201500507_sm_miscellaneous_information.pdf

Supporting Information

Computational Materials and Methods

Structural models. Three simulation systems of the COX-1 protein in complex with the arachidonic acid (AA) substrate, the flurbiprofen (FLP) and the ARN2508 compounds were built, namely COX-1/AA, COX-1/FLP and COX-1/ARN2508, respectfully. All model systems were based on the crystallographic structure of the sheep COX-1 in complex with AA bound in a chemically productive conformation, determined at 3.0 Å resolution (PDB code: 1DIY).¹ In this structure, Fe³⁺ of the HEME prostetic group has been substituted with Co³⁺ in order to create a native like COX-1 that lacks of both peroxidase and cyclooxygenase activity and does not form any prostaglandin product when incubated with AA. In our model systems, Co³⁺ has been replaced with Fe³⁺, in order to consistently reconstruct the biologically active Michaelis complexes. The crystallographic conformation of AA has been maintained as initial pose of our molecular dynamics (MD) simulations. Several x-ray structures of COX-1 in complex with FLP are available and provided the initial pose for FLP in the COX-1 active site.²⁻⁵ The initial binding mode of ARN2508 has been generated via computational docking of the ligand to the COX-1 binding site. Docking calculations were conducted using Glide SP.⁶ The three simulation systems were hydrated by means of a TIP3P water,⁷ and four K⁺ counterions were added to neutralize the total charge. The size of the final systems was approximately ~130 Å x ~103 Å x ~106 Å, with ~38,800 water molecules, resulting in a total number of ~135,000 atoms for each system. In the simulations, all the atoms of the COX-1 protein in complex with the AA, FLP and ARN2508, and water atoms were represented explicitly.

Molecular dynamics (MD) simulations. The all-atom AMBER/parm99⁸ force field was adopted for the COX-1 protein, whereas the AA, FLP and ARN2508 molecules were treated with the General Amber Force Field (GAFF)⁹ and the atomic charges were derived by the RESP fitting procedure.¹⁰ Parameters for the COX-1 high-spin ferric (Fe³⁺) HEME have been taken from Fernandez-Alberti et al.¹¹ The SHAKE¹² algorithm was used for all the covalent bonds that contain an H atom, thus allowing a timestep of 2 fs for the integration of the equations of motion. All simulations were performed by using the NAMD 2.9 package.^{11,13} Periodic boundary conditions were applied and the Particle-Mesh Ewald method was used to evaluate long-range electrostatic interactions with a direct cutoff of 10 Å. The simulations were performed with deprotonated AA, FLP and ARN2508, as assumed at physiological pH (~7.4). Standard protonation states were maintained for the protein residues. All the simulations were carried out with the following protocol. First, the systems were optimized and thermalized up to 300 K in the NVT *ensemble* using a Langevin bath,¹⁴ in three consecutive steps: (1) the solvent was first equilibrated, slowly increasing the temperature from 0 to 100 K and maintaining the protein fixed, (2) the temperature was further increased up to 200 K while keeping fixed only the coordinates of backbone atoms of the protein, (3) constraints were released and the systems were simulated to reach the temperature of 300 K. Subsequently, ~100 ns of MD were performed for each system in the NPT *ensemble* in standard condition using a Langevin Piston. Coordinates of the systems were collected every 2 ps, for a total of ~50,000 frames for each run. Statistics was accumulated during the last ~98 ns of each run. The structural analysis here reported is obtained using data from the two COX-1 monomers that form each complex, considered as independent, for a total of ~100,000 structures for each complex.

Binding free energy calculations. Binding free energies for the three ligands in the COX-1 protein were estimated by combining the Thermodynamic Cycle and MD simulations. This is a post-processing method in which representative snapshots from the *ensemble* of conformations are used to calculate the free energy change between two states (i.e., the bound and free state of the COX-1 protein and the ligands). The free energy is calculated by decomposing the contributions coming from the solvation energy from the reactants and products and from the binding free energy *in vacuo*. The MM/GB-PBSA (Molecular Mechanics/Generalized Born – Poisson Boltzmann Surface Area)¹⁵⁻¹⁷ method implemented in the Amber 12 package¹⁸ was used. This method has been shown to be an efficient computational approach for the estimation of the binding affinities in several protein/ligand complexes.^{19,20} Accordingly, the $\Delta G_{\text{Bind-GB/PB}}$ between a protein and a ligand to form a protein/ligand complex can be calculated as in eq [1].

$$\Delta G_{\text{Bind-GB/PB}} = \Delta E_{\text{MM}} + \Delta G_{\text{Sol}} - T\Delta S \quad [1]$$

$$\Delta E_{\text{MM}} = \Delta E_{\text{internal}} + \Delta E_{\text{electrostatic}} + \Delta E_{\text{vdW}} \quad [2]$$

$$\Delta G_{\text{Sol}} = \Delta G_{\text{SA}} + \Delta G_{\text{GB-PB}} \quad [3]$$

where ΔE_{MM} is the total gas phase energy, given by the sum of $\Delta E_{\text{internal}}$, $\Delta E_{\text{electrostatic}}$, ΔE_{vdW} . $\Delta E_{\text{internal}}$ is the internal energy arising from bond, angle and dihedral terms in the MM force field. $\Delta E_{\text{electrostatic}}$ and ΔE_{vdW} are the electrostatic and van der Waals contributions as calculated by the MM force field. ΔG_{Sol} is the sum of the nonpolar (ΔG_{NP}) and polar ($\Delta G_{\text{GB-PB}}$) contributions to the solvation free energy. $\Delta G_{\text{GB-PB}}$ is computed in continuum solvent, using the Poisson–Boltzmann model. ΔG_{SA} can be derived from the solvent-accessible surface area (SA). The last term in eq [1] ($T\Delta S$) is the conformational entropy upon binding computed by normal-mode analysis.

For the MM/GB-PBSA calculations, 5000 equally spaced snapshots of each of the COX-1/ligand complexes were extracted from the equilibrated MD trajectories (i.e., the last ~98 ns). In order to get uncorrelated structures, we extracted one snapshot every ~20 ps from all the six ~98 ns trajectories. All water molecules and counterions were removed before MM/GB-PBSA calculations. The dielectric constants $\epsilon = 1$ and $\epsilon = 80$ were used to reproduce the *in vacuo* and in solvent conditions, respectfully.

Analysis of structural data. We took the root-mean-square-deviation (RMSD) as stability parameter, after the equilibration time, with respect to the 1DIY crystal structure (Figures S1A).¹ After an transient period of ~2 ns, the RMSD for the all atoms of the protein settled at 3.28 ± 0.09 Å, 3.06 ± 0.17 Å, 3.45 ± 0.09 Å, for the COX-1/AA, COX-1/FLP and COX-1/ARN2508 systems, respectively. The RMSD for the protein heavy atoms confirmed that COX-1 conformation remained consistently stable throughout the simulations [RMSD = 2.49 ± 0.10 Å (COX-1/AA), 2.28 ± 0.18 Å (COX-1/FLP), 2.66 ± 0.30 Å (COX-1/ARN2508)]. The RMSD of the three AA, FLP and ARN2508 ligands remained below ~2 Å (Figure S1B). In detail, the RMSD of the AA was around 1.29 ± 0.20 Å in monomer A (Mnr-A) and 1.39 ± 0.22 Å in monomer B (Mnr-B). FLP and ARN2508 were highly stable during our simulations. Indeed, we detected RMSD values for FLP equal to 0.30 ± 0.16 Å (Mnr-A) and 0.57 ± 0.20 Å (Mnr-B), whereas in the case of ARN2508, the RMSD settled at 0.96 ± 0.17 Å (Mnr-A) and 0.88 ± 0.12 Å (Mnr-B).

During the equilibrium trajectories of the simulated systems, the interactions between the three ligands and the protein residues have been characterized by calculating the statistical distribution of the direct interactions (i.e., H-bonds and Hydrophobic contacts) between the AA, FLP and ARN2508 ligands and the COX-1 residues that in the 1DIY X-ray structure are in close contact to the natural AA substrate. In detail, the hydrogen bonds contacts between the COX-1 active site residues and the ligands were defined using cutoff values of 3.0 Å for acceptor–donor distance and 130° for acceptor–donor angle. Hydrophobic contacts were counted when nonpolar atoms were separated by at most 4.0 Å. The interaction network established the AA moieties in the X-ray structure has been taken as a reference for the analysis of the ligands binding, by defining the *carboxyl*, C_2 – C_{11} , C_{12} – C_{13} and C_{14} – C_{20} interaction regions (Figure 4, main text of this paper). Table S1 reports the full data. Due to the reproducibility of the results in both monomers, statistics was accumulated for the aggregate monomers on a total of sampling time of 200 ns (i.e., 200,000 frames) for each system. Table 1 reports statistical analysis for each separated monomer and the aggregate statistics.

Docking calculations. ARN2508 has been cocked within the COX-1 and FAAH active sites using the Glide²¹⁻²³ software of the Schrodinger suite.²⁴ Docking calculations have been performed considering the 1DIY.pdb¹ and the 1MT5.pdb²⁵ as target structures of COX-1 and FAAH binding, respectively. The protein/ligand systems were prepared with ProteinWizard.²⁴ The grid for the docking of ARN2508 was centered at the active site center level, while the maximum size of the docked ligands was set to 36 Å. For each docking calculation, we considered a maximum of 100 poses.

Supplementary Figures

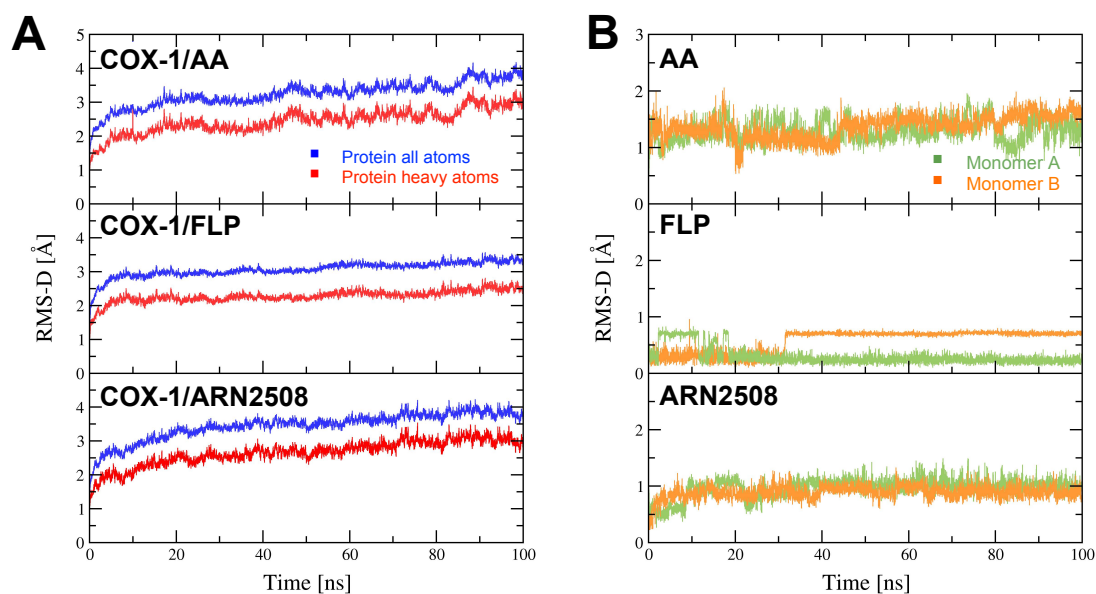


Figure S1. (A) Time evolution, along the MD trajectories of the COX-1/AA (upper graph), COX-1/FLP (central graph) and COX-1/ARN2508 (lower graph) systems, of the RMSD for the protein heavy atoms (red) and all-atoms (blue). (B) Time evolution along MD simulations of the RMSD for the AA (upper graph), FLP (central graph) and ARN2508 (lower graph) ligands within monomer A (green) and monomer B (orange) of the COX-1 protein.

Supplementary Tables

	Arg120	Tyr355	Glu524	Tyr348	Val349	Leu352	Trp387	Phe518
COX-1/AA – mnrA	12,4	14,0	0,5	5,8	23,0	40,5	11,3	17,4
COX-1/AA – mnrB	15,0	12,3	0,4	11,5	27,7	38,4	13,2	18,4
average	13,7	13,1	0,5	8,6	25,4	39,5	12,3	17,9
COX1/FLP – mnrA	16,9	21,3	0,1	4,1	41,4	34,8	14,0	11,4
COX1/FLP – mnrB	19,0	27,4	0,3	3,0	40,1	30,8	12,2	11,3
average	17,9	24,3	0,2	3,5	40,8	32,8	13,1	11,4
COX1/ARN – mnrA	16,2	23,8	0,1	20,0	38,4	30,9	13,2	10,2
COX1/ARN – mnrB	17,0	27,9	0,1	9,7	30,0	31,6	12,2	12,5
average	16,6	25,9	0,1	14,9	34,2	31,2	12,7	11,3

	Ser530	Tyr385	Phe205	Phe209	Val344	Phe381	Leu534	Ile523
COX-1/AA – mnrA	57,3	23,1	21,1	32,0	4,0	30,0	41,6	33,1
COX-1/AA – mnrB	48,4	24,2	19,4	30,4	10,6	27,9	38,9	39,7
average	52,8	23,7	20,2	31,2	7,3	29,0	40,3	36,4
COX1/FLP – mnrA	21,2	13,1	0,3	0,0	0,0	5,0	0,1	39,2
COX1/FLP – mnrB	21,6	13,8	1,7	0,0	0,1	5,8	0,2	35,2
average	21,4	13,5	1,0	0,0	0,1	5,4	0,2	37,2
COX1/ARN – mnrA	49,7	31,0	29,5	17,9	23,8	27,5	30,5	31,2
COX1/ARN – mnrB	42,4	25,1	20,4	39,5	6,5	25,8	38,5	25,1
average	46,0	28,1	25,0	28,7	15,1	26,6	34,5	28,1

Table S1. Statistical distribution (% of the total simulation time) of the direct interactions between COX-1 residues of monomer A (mnrA) monomer B (mnrB) and the AA, FLP and ARN2508 ligands. The aggregate results are reported as an average between the data arising from the two protein subunits.

References

- (1) Malkowski, M. G.; Ginell, S. L.; Smith, W. L.; Garavito, R. M. *Science* **2000**, *289*, 1933.
- (2) Gupta, K.; Selinsky, B. S.; Loll, P. J. *Acta Crystallogr. Sect. D* **2006**, *62*, 151.
- (3) Picot, D.; Loll, P. J.; Garavito, R. M. *Nature* **1994**, *367*, 243.
- (4) Selinsky, B. S.; Gupta, K.; Sharkey, C. T.; Loll, P. J. *Biochemistry* **2001**, *40*, 5172.
- (5) Sidhu, R. S.; Lee, J. Y.; Yuan, C.; Smith, W. L. *Biochemistry* **2010**, *49*, 7069.
- (6) Glide, v. S. d., LLC, New York, 2010.
- (7) Jorgensen, W. L.; Chandrasekhar, J.; Madura, J. D.; Impey, R. W.; Klein, M. L. *J Chem Phys* **1983**, *79*, 926
- (8) Cornell, W. D.; Cieplak, P.; Bayly, C. I.; Gould, I. R.; Merz, K. M.; Ferguson, D. M.; Spellmeyer, D. C.; Fox, T.; Caldwell, J. W.; Kollman, P. A. *J Am Chem Soc* **1995**, *117*, 5179.
- (9) Wang, J.; Wolf, R. M.; Caldwell, J. W.; Kollman, P. A.; Case, D. A. *J Comput Chem* **2004**, *25*, 1157.
- (10) Bayly, C. I.; Cieplak, P.; Cornell, W. D.; Kollman, P. A. *J Phys Chem* **1993** *97*, 10269.
- (11) Fernandez-Alberti, S.; Bacelo, D. E.; Binning, R. C., Jr.; Echave, J.; Chergui, M.; Lopez-Garriga, J. *Biophysical journal* **2006**, *91*, 1698.
- (12) Ryckaert, J. P.; Ciccotti, G.; Berendsen, H. J. C. *J Comput Phys* **1977**, *23*, 327.
- (13) Phillips, J. C.; Braun, R.; Wang, W.; Gumbart, J.; Tajkhorshid, E.; Villa, E.; Chipot, C.; Skeel, R. D.; Kale, L.; Schulten, K. *J Comput Chem* **2005**, *26*, 1781.
- (14) Feller, S. E.; Zhang, Y.; Pastor, R. W.; Brooks, R. W. *J Chem Phys* **1995**, *103*, 4613-4621.
- (15) Kuhn, B.; Gerber, P.; Schulz-Gasch, T.; Stahl, M. *Journal of medicinal chemistry* **2005**, *48*, 4040.
- (16) Kuhn, B.; Kollman, P. A. *Journal of medicinal chemistry* **2000**, *43*, 3786.
- (17) Miller, B. R. I.; Dwight McGee, T. J.; Swails, J. M.; Homeyer, N.; Gohlke, H.; Roitberg, A. E. *Journal of Chemical Theory and Computation* **2012**, *8*, 3314.
- (18) Case, D. A.; Darden, T. A.; Cheatham, T. E. I.; Simmerling, C. L.; Wang, J.; Duke, R. E.; Luo, R.; Walker, R. C.; Zhang, W.; Merz, K. M.; Roberts, B.; Hayik, S.; Roitberg, A.; Seabra, G.; Swails, J.; Goetz, A. W.; Kolossvai, I.; Wong, K. F.; Paesani, F.; Vanicek, J.; Wolf, R. M.; Liu, J.; Wu, X.; Brozell, S. R.; Steinbrecher, T.; Gohlke, H.; Cai, Q.; Ye, X.; Wang, J.; Hsieh, M.-J.; Cui, G.; Roe, D. R.; Mathews, D. H.; Seetin, M. G.; Salomon-Ferrer, R.; Sagui, C.; Babin, V.; Luchko, T.; Gusarov, S.; Kovalenko, A.; Kollman, P. A. *AMBER 12. San Francisco: University of California; 2012*. **2012**.
- (19) Collu, F.; Vargiu, A. V.; Dreier, J.; Cascella, M.; Ruggerone, P. *J Am Chem Soc* **2012**, *134*, 19146.
- (20) Srivastava, H. K.; Sastry, G. N. *J Chem Inf Model* **2012**, *52*, 3088.
- (21) Friesner, R. A.; Banks, J. L.; Murphy, R. B.; Halgren, T. A.; Klicic, J. J.; Mainz, D. T.; Repasky, M. P.; Knoll, E. H.; Shelley, M.; Perry, J. K.; Shaw, D. E.; Francis, P.; Shenkin, P. S. *J Med Chem* **2004**, *47*, 1739.
- (22) Friesner, R. A.; Murphy, R. B.; Repasky, M. P.; Frye, L. L.; Greenwood, J. R.; Halgren, T. A.; Sanschagrin, P. C.; Mainz, D. T. *J Med Chem* **2006**, *49*, 6177.
- (23) Halgren, T. A.; Murphy, R. B.; Friesner, R. A.; Beard, H. S.; Frye, L. L.; Pollard, W. T.; Banks, J. L. *J Med Chem* **2004**, *47*, 1750.
- (24) Sastry, G. M.; Adzhigirey, M.; Day, T.; Annabhimoju, R.; Sherman, W. *J Comput Aid Mol Des* **2013**, *27*, 221.
- (25) Bracey, M. H.; Hanson, M. A.; Masuda, K. R.; Stevens, R. C.; Cravatt, B. F. *Science* **2002**, *298*, 1793.